

Effects of high-boiling-point additive 2-Bromonaphthalene on polymer solar cells fabricated in ambient air

Xiaoxiang Sun¹ · Chang Li¹ · Like Huang¹ · Rui Xu¹ · Jian Ni¹ · Hongkun Cai¹ · Juan Li¹ · Jianjun Zhang¹

Received: 28 November 2016 / Revised: 22 February 2017 / Accepted: 3 March 2017 /
Published online: 9 March 2017
© Springer-Verlag Berlin Heidelberg 2017

Abstract High boiling point solvent additive, employed during the solution processing of active layer fabrications, impact the efficiency of bulk heterojunction polymer solar cells (PSC) by influencing the morphological of the active layer. The photovoltaic performances of the PSCs based on the donor of poly{4,8-bis[(2-ethylhexyl)oxy]benzo[1,2-b:4,5-b']-dithiophene-2,6-diyl-alt-3-fluoro-2-[(2-ethylhexyl)carbonyl] thieno[3,4-b]thiophene-4,6-diyl (PTB7) and the acceptor of [6, 6]-phenyl-C71-butyric-acidmethyl-ester (PC₇₁BM) was optimized using 5 vol% high-boiling-point solvent additive of 2-Bromonaphthalene (BN). The optimized air-processed PSC based on PTB7:PC₇₁BM (1:1.5 w/w) with 5 vol% BN exhibited a power conversion efficiency of 7.01% with open-circuit voltage (V_{oc}) of 0.731 V, short-circuit current density (J_{sc}) of 13.79 mA cm⁻², and fill factor (FF) of 69.46%. The effects of the additive on photovoltaic performances were illustrated with atomic force microscopy and transmission electron microscope measurements. Our results indicate that the improved efficiency is due to the optimized PTB7/PC₇₁BM interpenetrating network and the enhanced absorption of the active layer using the BN as solvent additive.

Keywords Morphology · Solvent additive · 2-Bromonaphthalene · High boiling point · Polymer solar cell

✉ Jian Ni
nijian_nankai@163.com

✉ Jianjun Zhang
jjzhang@nankai.edu.cn

¹ The Tianjin Key Laboratory for Optical-Electronics Thin Film Devices and Technology, College of Electronic Information and Optical Engineering, Nankai University, Tianjin 300071, China

Introduction

Nowadays, polymer solar cells (PSCs) have been widely studied by promising research groups due to their effective advantages such as light weight, low cost, high flexibility and simple fabrication processes [1–9]. Thanks to the development of new low bandgap donor polymers and better control of the nanoscale morphology of the interpenetrating electron donor–acceptor networks, great progress has been made in this field, and the power conversion efficiencies (PCEs) of solution-processed PSCs have reached 10–11% [10–13]. Various processing techniques have been developed to optimize the morphology of the bulk heterojunction (BHJ) material and to improve the PCE, including thermal annealing [14, 15], solvent annealing [16, 17], solvent vapor [18–20] and spontaneous interdiffusion of bilayer heterojunction [21, 22]. In addition, the use of additives has been recently demonstrated as an easy and efficient approach to modify and control the morphology of the active layer [23–25]. This technique is particularly interesting as it is compatible with extensive polymer systems and does not require extra processing steps. The addition of a small volume percent of solvent additive is able to significantly improve the PSCs performances in several polymeric systems by altering the morphological length scales of the donor and acceptor phases. A selective solubility to fullerene and a higher boiling point than the host solvent have been identified as two criteria for effective processing additive. The solvent additives effectively dissolve the [6]-phenyl-C₆₁-butyric acid methyl ester (PCBM) aggregate and promote the formation of smaller acceptor domains within the active layer [26–30]. High-boiling-point solvent additives, which employed during the solution processing of active-layer components, impact the efficiency of BHJ organic solar cells by influencing the morphological features of the multicomponent thin film [31–41]. The work carried out by Liang et al. showed that poly{4,8-bis[(2-ethylhexyl)oxy]benzo[1,2-b:4,5-b']-dithiophene-2,6-diyl-alt-3-fluoro-2-[(2-ethylhexyl)carbonyl]thieno[3,4-b]thiophene-4,6-diyl (PTB7): [6]-phenyl-C₇₁-butyric acid methyl ester (PC₇₁BM) (1:1.5) films prepared from dichlorobenzene (DCB) and 1,8-diiodooctane (DIO) (97%:3% in volume) increased the PCE from 6.22 to 7.18% comparison with the devices without DIO [42]. Guo et al. reported a PCE increment from 4.12 to 7.40% when 1-chloronaphthalene (CN) was used as the solvent additive based on poly(3-hexylthiophene) (P3HT): indene-C₇₀ bisadduct (IC₇₀BA) (1:1.5) films [43]. They observed the changes in the film morphology when additives were added in solvent. In this paper, a high boiling point solvent additive of 2-Bromonaphthalene (BN) was used to optimize the BHJ morphology and improved the device performances. As solvent additive, we used BN, which has a higher boiling-point (281 °C) than that of chlorobenzene (CB) (131.7 °C) [44]. The mixed CB/BN solvent may have a suitable volatilization speed for further PTB7 self-organization during solution-to-film transition stage. We have comprehensively studied the effects of various contents solvent additives BN on the BHJ PSCs based on PTB7:PC₇₁BM. Upon adding 5 vol% BN to the BHJ active layer, a PCE as high as 7.01% with a short-circuit current density (J_{sc}) of 13.79 mA cm⁻², fill factor (FF) of 69.46% and open-circuit voltage (V_{oc}) of 0.731 V is achieved. The techniques of

atomic force microscopy (AFM) and transmission electron microscope (TEM) have been applied to study the influence of BN on the morphology of the PTB7:PC₇₁BM blend. The results indicate that the optimum phase separation in BHJ film balances the charge transport between electron and hole and reduces bimolecular recombination, leading to an increase in PCE of the devices.

Experimental

All devices were fabricated and characterized in air, without protecting environment. The PSCs were fabricated with inverted structure of ITO/ZnO/active layer/WO₃/Ag, as shown in Fig. 1a. The chemical structure of PTB7, PC₇₁BM and solvent additive BN is shown in Fig. 1b. The patterned indium tin oxide (ITO) glass substrate was cleaned in detergent, water, acetone, and isopropyl alcohol under ultrasonication for 20 min. After ultraviolet/ozone treatment for 20 min, a thin layer (~50 nm) of ZnO ETL was prepared through spin coating at 2000 rpm from a ZnO precursor solution [45]. Then the ZnO substrate was annealed at 200 °C for 1 h in air. The PTB7 and PC₇₁BM (1:1.5 w/w) were co-dissolved in the mixed solvent of CB and BN (the content was varied from 0 to 7 vol%). The polymer concentration was 10 mg ml⁻¹ and the solution was stirred at 60 °C for 12 h under an atmosphere environment. Then the active layer (~100 nm) was spin-coated on the ZnO layer using the as-prepared solutions at 1500 rpm for 30 s in air. Finally, a 7-nm thick WO₃ layer and a 100-nm thick Ag layer were subsequently evaporated through a shadow mask (active area 6 mm²) under the pressure of 7.0 × 10⁻⁴ Pa.

The current density–voltage (*J*–*V*) characteristics of the devices were measured under 1 sun (AM 1.5G, 100 mW cm⁻²) simulator radiation. The surface morphologies were observed by AFM (Seiko SPA-400 SPM UNIT). TEM images were obtained using a Tecnai G² F20, the active layer on a PEDOT:PSS substrate was removed by dipping in DI water and then a holey carbon-coated copper grid

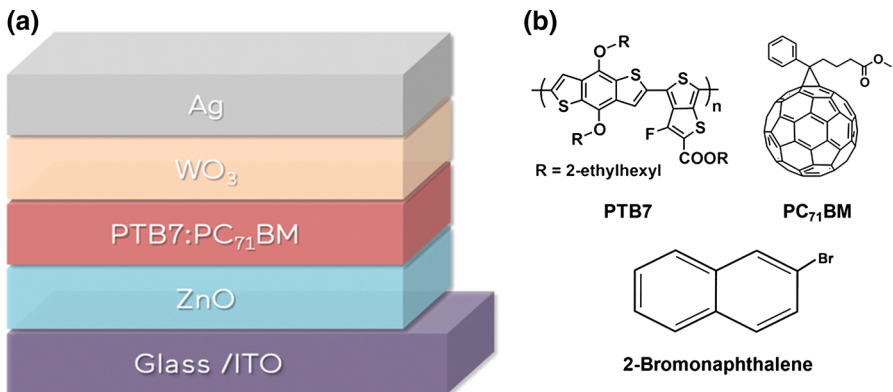


Fig. 1 a Architecture of inverted device: glass substrate/ITO/ZnO/PTB7:PC₇₁BM/WO₃/Ag. b Chemical structures of PTB7, PC₇₁BM and 2-Bromonaphthalene (BN)

was used to hold the film, which was dried in an oven at 50 °C. The absorption spectra of active layers were measured by spectrophotometer (Cary 5000 UV–VIS).

Results and discussion

The J – V characteristics of the PSCs prepared from adding various BN concentrations (0, 1, 3, 5, and 7 vol%) in CB solvent of BHJ solution are shown in Fig. 2a and the parameters of the devices are shown in Table 1. Without using BN, the V_{oc} is 0.752 V, but decreased as BN concentration increased. V_{oc} of PSCs decreased down to 0.730 V when 7 vol% BN is used as the processing additive [46]. However, in contrast to V_{oc} , the FF increased from 50.77 to 69.46% and then decreased to 66.69%. The J_{sc} of the devices increased from 10.46 mA cm⁻² (0 vol% BN) to 13.79 mA cm⁻² (5 vol% BN), but decreased to 12.57 mA cm⁻² when 7 vol% BN concentration is used. Table 1 shows the series resistances (R_s) and shunt resistances (R_{sh}) of the PSCs controlled the amount of BN. The R_s decreased from 16.3 Ω cm² (0 vol% BN) to 3.5 Ω cm² (5 vol%) and 7 vol% BN concentration (4.0 Ω cm²). On the other hand, the R_{sh} of the PSCs processed with BN increased from 0 vol% BN concentration (385 Ω cm²) to 3 vol% BN concentration (2633 Ω cm²) and 7 vol% BN concentration (749 Ω cm²). As the amount of BN added to the BHJ film increased, the R_s of PSCs decreased, and the R_{sh} of PSCs increased and became saturated. As a result, therefore, the PCE of the device without using BN is only 3.99%, and increased to 4.55% (with BN 1 vol%), and increased to 6.22% (with BN 3 vol%) and 7.01% (with BN 5 vol%), but decreased to 6.18% when 7 vol% BN was used. The variation of PCE is bound up with the V_{oc} , J_{sc} , and FF of devices, as seen in Fig. 3. The value of J_{sc} has been cross-checked with the integral of external quantum efficiency (EQE) spectrum and the results are within 5% error shown in Fig. 2b. In Fig. 2b, the EQE shows similar variation to J_{sc} of the PSCs with various BN concentrations. As the BN contents in the solvent were increased, the EQE of PSCs increased, and decreased to 7 vol% contents in solvent after reaching maximum in the BN 5 vol% condition. To analyze the optical

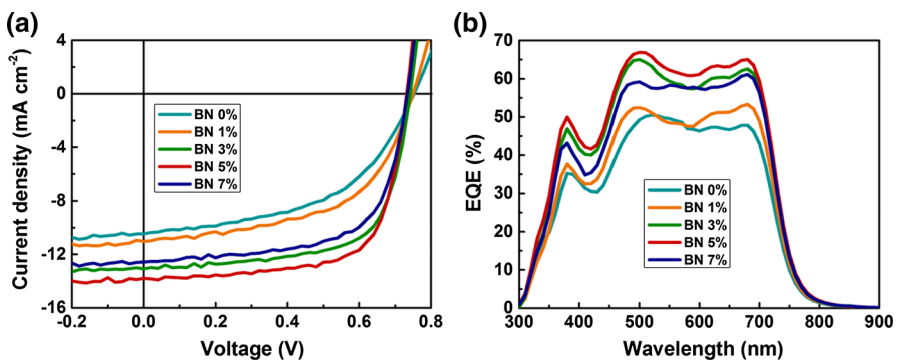
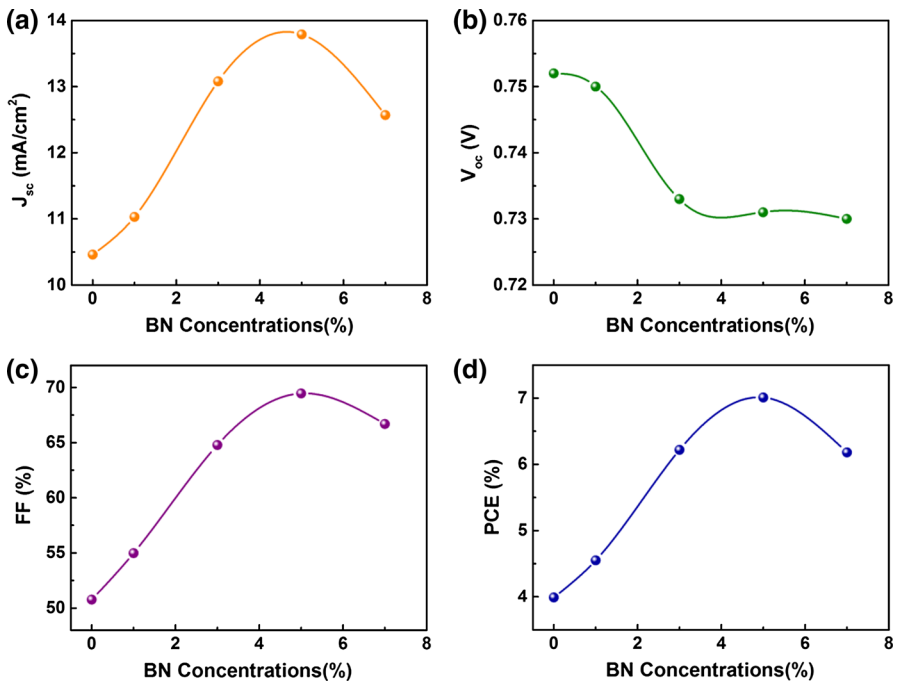


Fig. 2 Device performances of PTB7:PC₇₁BM with various BN concentrations (0, 1, 3, 5, and 7 vol%): **a** J – V characteristics of the PSCs under 1 sun illumination, **b** EQE of the PSCs

Table 1 The parameters of the BHJ solar cells prepared with various concentrations of BN additive

BN (vol%)	J_{sc} (mA cm ⁻²)	V_{oc} (V)	FF (%)	PCE (%)	R_S (Ω cm ²)	R_{Sh} (Ω cm ²)
0	10.46	0.752	50.77	3.99	16.3	385
1	11.03	0.750	54.98	4.55	11.2	516
3	13.08	0.733	64.78	6.22	4.0	1077
5	13.79	0.731	69.46	7.01	3.5	2633
7	12.57	0.730	66.69	6.18	4.1	749

**Fig. 3** a V_{oc} , b J_{sc} , c FF and d PCE of devices with different concentrations of BN

performance of active layer, the absorption spectra of PTB7:PC₇₁BM blend films with various BN concentrations (0, 1, 3, 5, and 7 vol%) measured are shown in Fig. 4. The absorption of the films with BN additive was significantly increased compared with that of films without BN additive, as shown in Fig. 4. Both EQE and absorption spectra of all these devices show a similar broad response covering a spectral range from 300 to 800 nm. With BN 5 vol% additive, the EQE and absorption spectra are lifted up [42].

To characterize the morphology of the PTB7:PC₇₁BM composite BHJ films with various BN contents in the solvent, we used AFM with tapping mode. For an accurate comparison with the device characteristic, all BHJ films were prepared under the same conditions as the PSC device preparation. Figure 5 shows the AFM

Fig. 4 Absorption spectra of PTB7:PC₇₁BM with various BN concentrations (0, 1, 3, 5, and 7 vol%)

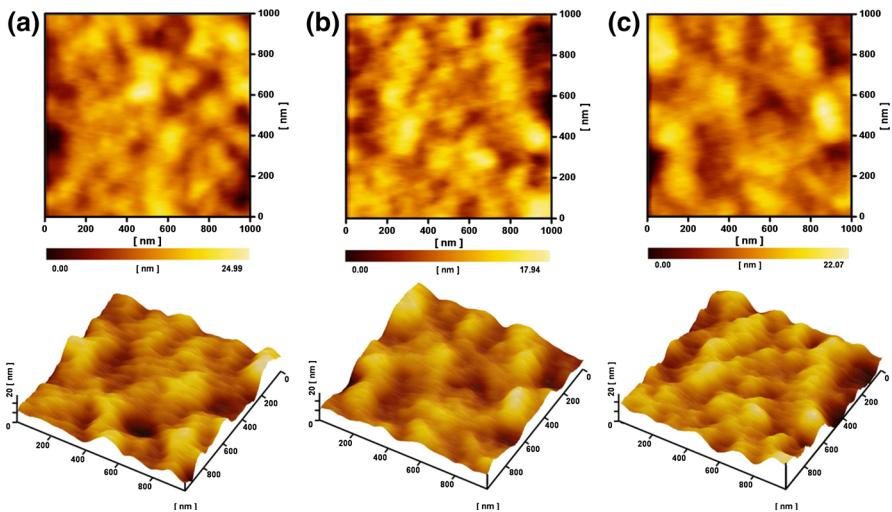
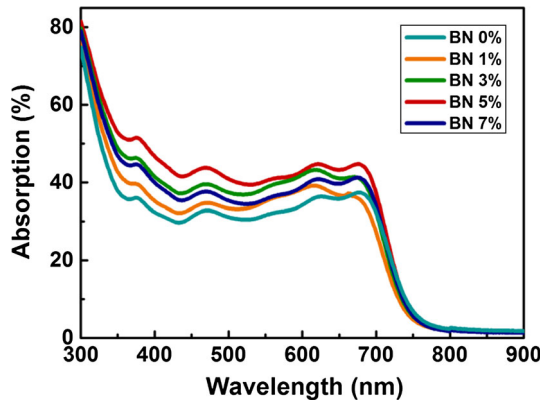


Fig. 5 AFM images of the PTB7:PC₇₁BM blend film with various BN concentrations **a** 0 vol%, **b** 5 vol%, and **c** 7 vol%

images of the BHJ films with various BN concentrations (0, 5 and 7 vol%) in the solvent. The root-mean-square (RMS) of the film without BN additives (Fig. 5a) is 3.9 nm, while that of the films with using additives of BN 5 and 7 vol% is 3.0 and 3.2 nm, respectively (Fig. 5b, c). Obviously, the surface roughness of the films becomes much smoother using the additives, and the surface of the film with BN 5 vol% additive shows the lower roughness. This indicates that the CB/BN solvent could adjust the miscibility between PTB7 and PC₇₁BM leading to the more homogeneous films [11, 47].

It has been approved that AFM images alone cannot provide unambiguous information regarding the structural properties in biphasic materials unless additional data are obtained by other techniques. Thus, TEM was performed to further investigate the effect of the additives on the interpenetrating networks of the

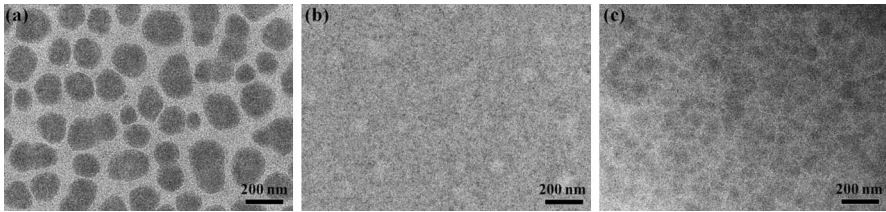


Fig. 6 TEM images of the PTB7:PC₇₁BM blend film with various BN concentrations **a** 0 vol%, **b** 5 vol%, and **c** 7 vol%

active layer. Figure 6 shows the TEM micrographs of approximately 100-nm thick active layer films under non-solvent additive and with BN solvent additives conditions. The micrograph of Fig. 6a shows large dimension clusters. These large dimensions are much greater than typical organic exciton diffusion lengths of ~ 10 nm, no doubt blocking the diffusion of exciton. When 5 vol% BN was added, as shown in Fig. 6b, we could observe the homogeneous distribution between PTB7 and PC₇₁BM. In this condition, the large aggregated PC₇₁BM could be removed fully and the PC₇₁BM could integrate into the PTB7 aggregates. Due to the large difference in vapor pressure, the final film morphology was essentially determined by the slow evaporation of BN. Its low vapor pressure, and therefore, reduced evaporation, retards the solidification of PC₇₁BM [48]. On the other hand, the uniform interpenetrating networks of PTB7:PC₇₁BM is beneficial to the exciton diffusion. The interpenetrating networks with phase-separated domains in the active layer apparently provide not only interfaces for charge separation of photo-generated excitons but also percolation pathways for charge carrier transport to the respective electrodes, which can critically affect the performance of devices [49, 50]. However, when the BN was added to the active layer in a more than optimized condition (7 vol%), we could observe that the BHJ film start to coarsened again. Our results indicate that with large domains come a low interfacial area and correspondingly small J_{sc} . In other words, the tuning ability of BN and thus the morphology of the resulting film depend on the BN percentage. With an optimal BN content, a significantly increased of PCE may be realized giving rise to an interpenetrating network of polymer and fullerene.

Conclusions

In summary, we have investigated the morphology and device performance relation of BHJ solar cells based on the donor of PTB7 and the acceptor of PC₇₁BM. By adding a suitable of BN additive (5 vol%) to the host solvent CB, the PCE was improved from 3.99 to 7.01%. The enhancement in PCE is due to the optimized PTB7:PC₇₁BM interpenetrating network and the stronger absorption of the active layer caused by the solvent additive.

Acknowledgements This work was supported by National Natural Science Foundation of China (Grant No. 61377031) and the National Natural Science Foundation of China (No. 61404073).

References

1. Szarko JM, Guo J, Liang Y, Lee B, Rolczynski BS, Strzalka J, Xu T, Loser S, Marks TJ, Yu L (2010) When function follows form: effects of donor copolymer side chains on film morphology and BHJ solar cell performance. *Adv Mater* 22:5468–5472
2. Lu L, Zheng T, Wu Q, Schneider AM, Zhao D, Yu L (2015) Recent advances in bulk heterojunction polymer solar cells. *Chem Rev* 115:12666–12731
3. Krebs FC, Gevorgyan SA, Alstrup J (2009) A roll-to-roll process to flexible polymer solar cells: model studies, manufacture and operational stability studies. *J Mater Chem* 19:5442–5451
4. Li C, Liu M, Pschirer NG, Baumgarten M, Müllen K (2010) Polyphenylene-based materials for organic photovoltaics. *Chem Rev* 110:6817–6855
5. Dennler G, Scharber MC, Brabec CJ (2009) Polymer-fullerene bulk-heterojunction solar cells. *Adv Mater* 21:1323–1338
6. Forrest SR (2004) The path to ubiquitous and low-cost organic electronic appliances on plastic. *Nature* 428:911–918
7. Zeng W, Song G, Li Y, Yuan C, Fan T, Tang W, Wang J, Zhao C, Lai W, Zhang H (2016) Enhanced performance of poly (3-hexylthiophene-2, 5-diyl):[6, 6]-phenyl-C61-butiric acid methyl ester solar cells by UV irradiation. *Thin Solid Films* 600:136–141
8. Zhou Y, Shim JW, Fuentes-Hernandez C, Khan TM, Kippelen B (2014) Inverted organic solar cells with polymer-modified fluorine-doped tin oxide as the electron-collecting electrode. *Thin Solid Films* 554:54–57
9. Qi L, Zhang C, Chen Q (2014) Performance improvement of inverted organic solar cells by adding ultrathin Al₂O₃ as an electron selective layer and a plasma enhanced chemical vapor deposition of SiO_x encapsulating layer. *Thin Solid Films* 567:1–7
10. He Z, Xiao B, Liu F, Wu H, Yang Y, Xiao S, Wang C, Russell TP, Cao Y (2015) Single-junction polymer solar cells with high efficiency and photovoltage. *Nat Photonics* 9:174–179
11. Zhao J, Li Y, Yang G, Jiang K, Lin H, Ade H, Ma W, Yan H (2016) Efficient organic solar cells processed from hydrocarbon solvents. *Nat Energy* 1:15027
12. Etxebarria I, Ajuria J, Pacios R (2015) Solution-processable polymeric solar cells: a review on materials, strategies and cell architectures to overcome 10%. *Org Electron* 19:34–60
13. Vohra V, Kawashima K, Kakara T, Koganezawa T, Osaka I, Takimiya K, Murata H (2015) Efficient inverted polymer solar cells employing favourable molecular orientation. *Nat Photonics* 9:403–408
14. Ma W, Yang C, Gong X, Lee K, Heeger AJ (2005) Thermally stable, efficient polymer solar cells with nanoscale control of the interpenetrating network morphology. *Adv Funct Mater* 15:1617–1622
15. Yang X, Loos J, Veenstra SC, Verhees WJ, Wienk MM, Kroon JM, Michels MA, Janssen RA (2005) Nanoscale morphology of high-performance polymer solar cells. *Nano Lett* 5:579–583
16. Li G, Shrotriya V, Huang J, Yao Y, Moriarty T, Emery K, Yang Y (2005) High-efficiency solution processable polymer photovoltaic cells by self-organization of polymer blends. *Nat Mater* 4:864–868
17. Li G, Yao Y, Yang H, Shrotriya V, Yang G, Yang Y (2007) “Solvent annealing” effect in polymer solar cells based on poly (3-hexylthiophene) and methanofullerenes. *Adv Funct Mater* 17:1636–1644
18. Fukuda T, Toda A, Takahira K, Suzuki K, Liao Y, Hirahara M, Saito M, Osaka I (2016) Molecular ordering of spin-coated and electrosprayed P3HT: PCBM thin films and their applications to photovoltaic cell. *Thin Solid Films* 612:373–380
19. Wu FC, Li YH, Tsou CJ, Tung KC, Yen CT, Chou FS, Tang FC, Chou WY, Ruan J, Cheng HL (2015) Synergistic effects of binary-solvent annealing for efficient polymer-fullerene bulk heterojunction solar cells. *ACS Appl Mater Interfaces* 7:18967–18976
20. Wang D, Zhang F, Li L, Yu J, Wang J, An Q, Tang W (2014) Tuning nanoscale morphology using mixed solvents and solvent vapor treatment for high performance polymer solar cells. *RSC Adv* 4:48724–48733
21. Moon JS, Takacs CJ, Sun Y, Heeger AJ (2011) Spontaneous formation of bulk heterojunction nanostructures: multiple routes to equivalent morphologies. *Nano Lett* 11:1036–1039
22. Wang DH, Moon JS, Seifert J, Jo J, Park JH, Park OO, Heeger AJ (2011) Sequential processing: control of nanomorphology in bulk heterojunction solar cells. *Nano Lett* 11:3163–3168
23. Peet J, Kim JY, Coates NE, Ma WL, Moses D, Heeger AJ, Bazan GC (2007) Efficiency enhancement in low-bandgap polymer solar cells by processing with alkane dithiols. *Nat Mater* 6:497–500
24. Yao Y, Hou J, Xu Z, Li G, Yang Y (2008) Effects of solvent mixtures on the nanoscale phase separation in polymer solar cells. *Adv Funct Mater* 18:1783–1789

25. Moon JS, Takacs CJ, Cho S, Coffin RC, Kim H, Bazan GC, Heeger AJ (2010) Effect of processing additive on the nanomorphology of a bulk heterojunction material†. *Nano Lett* 10:4005–4008
26. Demeshko S, Dechert S, Meyer F (2004) Anion- π interactions in a carousel copper (II)-triazene complex. *J Am Chem Soc* 126:4508–4509
27. Schottel BL, Chifotides HT, Dunbar KR (2008) Anion- π interactions. *Chem Soc Rev* 37:68–83
28. Chaban VV, Maciel C, Fileti EE (2014) Does the like dissolves like rule hold for fullerene and ionic liquids? *J Solut Chem* 43:1019–1031
29. Hedley GJ, Ward AJ, Alekseev A, Howells CT, Martins ER, Serrano LA, Cooke G, Ruseckas A, Samuel ID (2013) Determining the optimum morphology in high-performance polymer-fullerene organic photovoltaic cells. *Nat Commun* 4:1–10
30. Liu X, Huettner S, Rong Z, Rong Z, Friend RH (2012) Solvent additive control of morphology and crystallization in semiconducting polymer blends. *Adv Mater* 24:669–674
31. van Duren JK, Yang X, Loos J, Bulle-Lieuwma CW, Sieval AB, Hummelen JC, Janssen RA (2004) Relating the morphology of poly (p-phenylene vinylene)/methanofullerene blends to solar-cell performance. *Adv Funct Mater* 14:425–434
32. Shaheen SE, Brabec CJ, Sariciftci NS, Padinger F, Fromherz T, Hummelen JC (2001) 2.5% efficient organic plastic solar cells. *Appl Phys Lett* 78:841–843
33. Hoppe H, Glatzel T, Niggemann M, Schwinger W, Schaeffler F, Hinsch A, Lux-Steiner MC, Sariciftci N (2006) Efficiency limiting morphological factors of MDMO-PPV: PCBM plastic solar cells. *Thin Solid Films* 511:587–592
34. Padinger F, Rittberger RS, Sariciftci NS (2003) Effects of postproduction treatment on plastic solar cells. *Adv Funct Mater* 13:85–88
35. Kim Y, Cook S, Tuladhar SM, Choulis SA, Nelson J, Durrant JR, Bradley DD, Giles M, McCulloch I, Ha C-S (2006) A strong regioregularity effect in self-organizing conjugated polymer films and high-efficiency polythiophene: fullerene solar cells. *Nat Mater* 5:197–203
36. Zhang F, Jespersen KG, Björström C, Svensson M, Andersson MR, Sundström V, Magnusson K, Moons E, Yartsev A, Inganäs O (2006) Influence of solvent mixing on the morphology and performance of solar cells based on polyfluorene copolymer/fullerene blends. *Adv Funct Mater* 16:667–674
37. Chen LM, Hong Z, Li G, Yang Y (2009) Recent progress in polymer solar cells: manipulation of polymer: fullerene morphology and the formation of efficient inverted polymer solar cells. *Adv Mater* 21:1434–1449
38. Hoven CV, Dang XD, Coffin RC, Peet J, Nguyen TQ, Bazan GC (2010) Improved performance of polymer bulk heterojunction solar cells through the reduction of phase separation via solvent additives. *Adv Mater* 22:E63–E66
39. Lee JK, Ma WL, Brabec CJ, Yuen J, Moon JS, Kim JY, Lee K, Bazan GC, Heeger AJ (2008) Processing additives for improved efficiency from bulk heterojunction solar cells. *J Am Chem Soc* 130:3619–3623
40. Pivrikas A, Stadler P, Neugebauer H, Sariciftci NS (2008) Substituting the postproduction treatment for bulk-heterojunction solar cells using chemical additives. *Org Electron* 9:775–782
41. Moulé AJ, Meerholz K (2008) Controlling morphology in polymer–fullerene mixtures. *Adv Mater* 20:240–245
42. Liang Y, Xu Z, Xia J, Tsai ST, Wu Y, Li G, Ray C, Yu L (2010) For the bright future—bulk heterojunction polymer solar cells with power conversion efficiency of 7.4%. *Adv Mater* 22:135–138
43. Guo X, Cui C, Zhang M, Huo L, Huang Y, Hou J, Li Y (2012) High efficiency polymer solar cells based on poly (3-hexylthiophene)/indene-C70 bisadduct with solvent additive. *Energy Environ Sci* 5:7943–7949
44. Turro NJ, Bolt JD, Kuroda Y, Tabushi I (1982) A study of the kinetics of inclusion of halonaphthalenes with β -cyclodextrin via time correlated phosphorescence. *Photochem Photobiol* 35:69–72
45. Sun X, Ni J, Li C, Huang L, Xu R, Li Z, Cai H, Li J, Zhang J (2016) Air-processed high performance ternary blend solar cell based on PTB7-Th: PCDTBT: PC₇₀BM. *Org Electron* 37:222–227
46. Kim W, Kim JK, Kim E, Ahn TK, Wang DH, Park JH (2015) Conflicted effects of a solvent additive on PTB7: PC₇₁BM bulk heterojunction solar cells. *J Phys Chem C* 119:5954–5961
47. Huo L, Liu T, Sun X, Cai Y, Heeger AJ, Sun Y (2015) Single-junction organic solar cells based on a novel wide-bandgap polymer with efficiency of 9.7%. *Adv Mater* 27:2938–2944
48. Liu F, Zhao W, Tumbleston JR, Wang C, Gu Y, Wang D, Briseno AL, Ade H, Russell TP (2014) Understanding the morphology of PTB7: PCBM blends in organic photovoltaics. *Adv Energy Mater* 4:1301377

49. Hendriks KH, Heintges GH, Gevaerts VS, Wienk MM, Janssen RA (2013) High-molecular-weight regular alternating diketopyrrolopyrrole-based terpolymers for efficient organic solar cells. *Angew Chem Int Ed* 52:8341–8344
50. Li W, Hendriks KH, Furlan A, Roelofs WC, Wienk MM, Janssen RA (2013) Universal correlation between fibril width and quantum efficiency in diketopyrrolopyrrole-based polymer solar cells. *J Am Chem Soc* 135:18942–18948